



Cite this: *Phys. Chem. Chem. Phys.*,
2022, 24, 18169

Ozone production in electron irradiated CO₂:O₂ ices

Duncan V. Mifsud, ^{*ab} Zuzana Kaňuchová, ^{*c} Sergio Ioppolo, ^{*d} Péter Herczku, ^{*b} Alejandra Traspas Muiña, ^d Béla Sulik, ^b K. K. Rahul, ^b Sándor T. S. Kovács, ^b Perry A. Hailey, ^a Robert W. McCullough, ^e Nigel J. Mason ^{*a} and Zoltán Juhász ^{*b}

The detection of ozone (O₃) in the surface ices of Ganymede, Jupiter's largest moon, and of the Saturnian moons Rhea and Dione, has motivated several studies on the route of formation of this species. Previous studies have successfully quantified trends in the production of O₃ as a result of the irradiation of pure molecular ices using ultraviolet photons and charged particles (*i.e.*, ions and electrons), such as the abundances of O₃ formed after irradiation at different temperatures or using different charged particles. In this study, we extend such results by quantifying the abundance of O₃ as a result of the 1 keV electron irradiation of a series of 14 stoichiometrically distinct CO₂:O₂ astrophysical ice analogues at 20 K. By using mid-infrared spectroscopy as our primary analytical tool, we have also been able to perform a spectral analysis of the asymmetric stretching mode of solid O₃ and the variation in its observed shape and profile among the investigated ice mixtures. Our results are important in the context of better understanding the surface composition and chemistry of icy outer Solar System objects, and may thus be of use to future interplanetary space missions such as the *ESA Jupiter Icy Moons Explorer* and the *NASA Europa Clipper* missions, as well as the recently launched *NASA James Webb Space Telescope*.

Received 2nd April 2022,
Accepted 9th July 2022

DOI: 10.1039/d2cp01535h

rsc.li/pccp

1 Introduction

Ozone (O₃) plays an important role in planetary chemistry. On Earth, gaseous O₃ is located in the stratosphere and serves as an excellent absorber of short-wavelength ($\lambda = 200\text{--}315\text{ nm}$) ultraviolet photons known to cause damage to biomolecules, and thus has important implications for the development and sustenance of life on the planet.¹ In the solid phase, icy O₃ has been detected on the surfaces of several outer Solar System moons such as Ganymede in the Jovian system and Rhea and Dione in the Saturnian system,^{2,3} where it is thought to be an active participant in surface chemistry by virtue of its potent oxidising nature.⁴ Conversely, O₃ has not been detected in

some of the most well-studied comets, such as 1P/Halley and 67P/Churyumov-Gerasimenko, despite relatively high abundances of O₂ having been detected in their comae.^{5,6}

A good understanding of the astrochemical reactions leading to the production of O₃ is thus integral to better constraining the chemistry of planetary, lunar, and other Solar System bodies. Accordingly, several laboratory experiments have been performed to explore the formation of O₃ as a result of the irradiation of astrophysical molecular ice analogues using ultraviolet photons and charged particles (*i.e.*, ions and electrons). Perhaps the best studied of these ices is O₂, whose irradiation by ultraviolet photons, ions, and electrons has been studied extensively and has been shown to produce high yields of O₃.^{7–15}

Such experiments have demonstrated the dependence of O₃ formation in irradiated O₂ ices on a number of experimental parameters. For instance, Sivaraman *et al.*⁸ demonstrated that lower temperatures are more conducive to the formation of O₃ due to higher recombination rates of radiolytically derived oxygen atoms to reform O₂ at higher temperatures, thus leaving fewer atoms available to react with O₂ and produce O₃. Interestingly, there appears to be no dependence of the O₃ yield on the dose supplied or the mass of the incident irradiating particle, with irradiations of solid O₂ using mono-energetic electrons, protons, and helium, carbon, nitrogen, and oxygen

^a Centre for Astrophysics and Planetary Science, School of Physical Sciences, University of Kent, Canterbury CT2 7NH, UK. E-mail: dm618@kent.ac.uk, n.j.mason@kent.ac.uk

^b Institute for Nuclear Research (Atomki), Debrecen H-4026, Hungary. E-mail: herczku@atomki.hu, zjuhasz@atomki.hu

^c Astronomical Institute, Slovak Academy of Sciences, Tatranská Lomnica SK-059 60, Slovakia. E-mail: zkanuch@ta3.sk

^d School of Electronic Engineering and Computer Science, Queen Mary University of London, London E1 4NS, UK. E-mail: s.ioppolo@qmul.ac.uk

^e Department of Physics and Astronomy, School of Mathematics and Physics, Queen's University Belfast, Belfast BT7 1NN, UK



ions all showing that a similar abundance of O_3 is produced after a given fluence in each case.^{7,9,11} This has been attributed to inelastic stopping interactions being the dominant mechanism of energy transfer in the O_2 ice, as all these charged projectiles possess linear energy transfer values which are on the same order of magnitude.

Attention has also been paid to the radiation-induced formation of O_3 from molecular ices other than O_2 , such as CO_2 .^{9,16–21} Here, O_3 is produced as a result of a three-step process which requires that sufficient O_2 is first accumulated within the structure of the ice. Temperature has been noted to play a role in this radiolytic chemistry, with increased yields of O_3 being recorded on increasing the reaction temperature from 20 to 40 K.²¹ On raising the temperature further, however, the total yield of O_3 was noted to decline due to increased sublimation-induced losses of the necessary O_2 precursor molecules.^{16,21}

In this paper, we present the results of a systematic study of the 1 keV electron irradiation of a series of 14 stoichiometrically distinct CO_2 : O_2 molecular ices at 20 K, including the two pure end-members. The composition of these ices is particularly relevant to studies of different icy outer Solar System bodies.²² For example, these species are known to be constituents of the icy nuclei of comets.^{23,24} Furthermore, the detection of a tenuous exosphere on the Saturnian moon Rhea composed primarily of CO_2 and O_2 has led to the suggestion that it is sourced from sputtered or de-gassed surface ices.²⁵ Such icy outer Solar System bodies are exposed to ionising radiation in the form of the solar wind and giant planetary magnetospheric plasmas. As such, laboratory irradiations of CO_2 : O_2 astrophysical ice analogues are well suited to understanding the chemistry of such celestial bodies.

In this study, we have used mid-infrared spectroscopy to quantify the production efficiency of O_3 from the electron irradiated CO_2 : O_2 ices; as well as to determine how the appearance of its mid-infrared asymmetric stretching (ν_3) band varies according to the initial stoichiometric composition of the ice. Understanding such variations is particularly important in light of the fact that O_3 is often used as a marker molecule for the presence of O_2 , which is more difficult to confirm *via* direct spectroscopic observations. Such spectroscopic work could thus greatly aid in the interpretation of data collected by forthcoming interplanetary missions, such as the ESA *Jupiter Icy Moons Explorer* and the NASA *Europa Clipper* missions.^{26,27} The recently launched NASA *James Webb Space Telescope* is also anticipated to generate large data-sets of mid-infrared spectroscopic measurements of icy outer Solar System bodies,²⁸ and so could also aid in the detection of O_3 in the surface ices of those bodies.

2 Experimental methodology

Experimental work was performed using the Ice Chamber for Astrophysics-Astrochemistry (ICA) located at the Institute for Nuclear Research (Atomki) in Debrecen, Hungary. This set-up has been described in great detail in previous publications,^{29,30}

and so only the most salient features will be presented here. The ICA is an ultra-high vacuum compatible chamber containing a gold-coated sample holder hosting a series of ZnSe deposition substrates which may be cooled to 20 K by a closed-cycle helium cryostat. The temperature of the substrates may be regulated within the 20–300 K range and is measured using two silicon diodes. The pressure in the chamber is typically maintained at a few 10^{-9} mbar *via* the combined use of a dry rough vacuum pump and a turbomolecular pump.

The preparation of CO_2 : O_2 astrophysical ice analogues onto the ZnSe substrates was performed *via* background deposition of dosed gases at 20 K. First, CO_2 and O_2 (both Linde Minican; 99.995%) were introduced into a pre-mixing chamber in the desired stoichiometric ratio, which was determined through standard manometric practices. After being left to equilibrate within the pre-mixing chamber for a few minutes, the gas mixture was dosed into the main chamber *via* an all-metal needle valve at a pressure of a few 10^{-6} mbar. Deposition could be followed *in situ* using Fourier-transform mid-infrared transmission absorption spectroscopy (spectral range = 4000–650 cm^{-1} ; spectral resolution = 1 cm^{-1}).

In principle, the thickness d (μm) of a deposited astrophysical ice analogue may be determined spectroscopically by first calculating its molecular column density N (molecules cm^{-2}) *via* a modified version of the Beer–Lambert Equation (eqn (1)), and subsequently using this value for N in eqn (2):²⁹

$$N = \frac{1}{A_\nu} \int \tau(\nu) d\nu \quad (1)$$

$$d = \frac{NZ}{\rho N_A} \times 10^4 \quad (2)$$

where A_ν is the integrated band strength constant (cm molecule^{-1}) of the mid-infrared absorption band over which eqn (1) is integrated, $\tau(\nu)$ is the optical depth of the ice (cm^{-1}), Z is the mass of the molecular constituent whose absorption band was integrated over (g mol^{-1}), ρ is the density of the ice (g cm^{-3}), and N_A is the Avogadro constant (6.02×10^{23} molecule mol^{-1}). Eqn (1) and (2) are valid for pure ices, although their extrapolation to mixed ices is straightforward.^{29,30} However, this assumes that all ices in the mixture are infrared active and present absorption bands which may be integrated over.

However, being a homonuclear diatomic molecule, O_2 is infrared inactive. Its weak spectral absorption features related to the O–O stretching mode cannot be used to reliably and quantitatively determine the thickness of an ice due to the rather extreme variations in the value of A_ν reported in the literature (for a more complete discussion, see the work of Bennett and Kaiser⁷). Therefore, eqn (1) and (2) cannot be used to determine the stoichiometric compositions and thicknesses of our CO_2 : O_2 astrophysical ice analogues. Nevertheless, we are able to provide a reasonable estimate of these parameters for our deposited ices based on the known mixing ratio of the gases in the pre-mixing chamber, as well as quadrupole mass spectrometric measurements of the CO_2 and O_2 integrated signal curves for the gas mixtures dosed into the main chamber.



Table 1 Estimated stoichiometric compositions and thicknesses of the studied ices irradiated by 1 keV electrons

Ice	CO ₂ :O ₂ ratio	Estimated molecular column density (10 ¹⁷ molecules cm ⁻²)		% content		Estimated ice thickness (μm)
		CO ₂	O ₂	CO ₂	O ₂	
1	1:0	6.38	—	100	0	0.48
2	73:5	7.25	0.50	94	6	0.56
3	53:10	7.36	1.39	84	16	0.60
4	14:5	6.90	2.47	74	26	0.60
5	2:1	7.21	3.61	67	33	0.66
6	7:5	6.03	4.31	58	42	0.60
7	1:1	4.10	4.09	50	50	0.45
8	5:6	3.17	3.81	45	55	0.37
9	2:5	1.92	4.80	29	71	0.31
10	5:14	1.23	3.46	26	74	0.21
11	1:5	1.02	5.08	17	83	0.25
12	1:6	1.12	6.71	14	86	0.31
13	1:50	0.41	20.69	2	98	0.75
14	0:1	—	15.90	0	100	0.55

We have been able to determine the thickness of the CO₂ component of our deposited mixed ices by integrating eqn (1) over the asymmetric stretching mode (ν_3) at 2344 cm⁻¹ and taking A_{ν_3} to be 7.6×10^{-17} cm molecule⁻¹^{21,31} before using eqn (2) and taking ρ to be 0.98 g cm⁻³.³² By taking ρ to be 1.54 g cm⁻³ for O₂ ice,³³ and in combination with our spectrometric estimates of the compositions of the deposited ices, we have estimated the total thicknesses of our ices to be in the range 0.20–0.75 μm.

In total, a series of 14 stoichiometrically distinct CO₂:O₂ ices were deposited onto the ZnSe substrates (Table 1). Once deposited, a mid-infrared absorption spectrum of the ice was collected after which the ice was irradiated using 1 keV electrons at an incidence angle of 36° to the normal. Prior to commencing the experiment, the electron beam current and profile were quantified using the method described previously by Mifsud *et al.*³⁰ Our use of a 1 keV electron beam is not only representative of irradiation processes occurring in astrophysical environments such as icy outer Solar System moons, but is also similar to electron beam energies used in previous studies of radiation ice astrochemistry hence allowing for more meaningful comparisons to be made.

The electron beam was scanned over an area of 0.9 cm², which represents >80% of the area scanned by the mid-infrared spectroscopic beam.²⁹ Each ice was irradiated for a total of 50 minutes using beam fluxes of $2.0\text{--}2.4 \times 10^{13}$ e⁻ cm⁻² s⁻¹, corresponding to total delivered fluences of $6.0\text{--}7.2 \times 10^{16}$ e⁻ cm⁻². The penetration depths of a 1 keV electron in pure CO₂ and O₂ ices was calculated using the CASINO software³⁴ and were found to be 65 and 44 nm, respectively (Fig. 1). Given our estimates for the thicknesses of our ices, it may be stated that the incident electrons were effectively implanted into the ice.

3 Results and discussion

Mid-infrared spectra of the pure CO₂ and O₂ molecular ices, as well as of the 1:1 binary ice, both before and after 1 keV

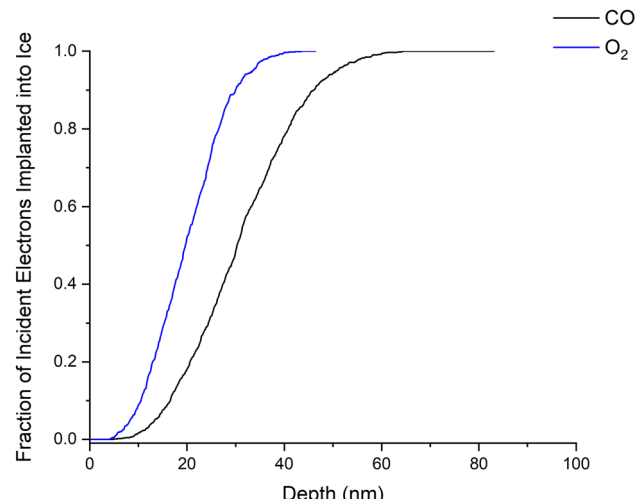


Fig. 1 CASINO simulations of the maximum penetration depths of 1 keV electrons in pure CO₂ (black trace; 65 nm) and pure O₂ (blue trace; 44 nm) ices. Maximum penetration depths for the mixed CO₂:O₂ ices lie within this range at a value that depends on the stoichiometric composition of the ice. Simulations were performed using an incidence angle of 36° to the normal and using density values of 0.98 and 1.54 g cm⁻³ for CO₂ and O₂, respectively.^{32,33}

electron irradiation, are presented in Fig. 2. The onset of irradiation results in the development of new absorption bands due to the formation of new molecules driven by a cascade of tens of thousands of low-energy (<20 eV) secondary electrons.^{35,36} The presence of O₃ as a radiolytic product was confirmed in each of the investigated ices *via* the detection of its characteristic asymmetric stretching mode (ν_3) at about 1040 cm⁻¹. In the mid-infrared region, O₃ presents one combination and three fundamental absorption bands:^{9,37–39} a bending mode (ν_2) at about 700 cm⁻¹, the asymmetric stretching mode (ν_3) at 1040 cm⁻¹, a symmetric stretching mode (ν_1) at 1125 cm⁻¹, and a combination mode ($\nu_1 + \nu_3$) at 2100 cm⁻¹.

The radiation chemistry leading to the formation of O₃ from irradiated O₂ and CO₂ ices is straightforward and begins with their electron impact dissociation to yield a supra-thermal oxygen atom (eqn (3) and (4)).^{40,41} In pure O₂ ices, this oxygen atom then combines with a O₂ molecule to directly yield O₃ (eqn (5)). In the case of pure CO₂ ices, the production of O₃ is the result of a three-step process which first requires that a sufficient number of oxygen atoms combine to give O₂ (eqn (6)), after which the addition of another oxygen atom furnishes the O₃ product (eqn (5)). The addition of atomic oxygen to O₂ has traditionally been considered to be energetically barrierless,^{7,8} although Ioppolo *et al.* have proposed a small activation energy barrier of <0.05 eV.⁴²



The shape and profile of the O₃ asymmetric stretching mode (ν_3) used for its spectroscopic identification offers a chemical



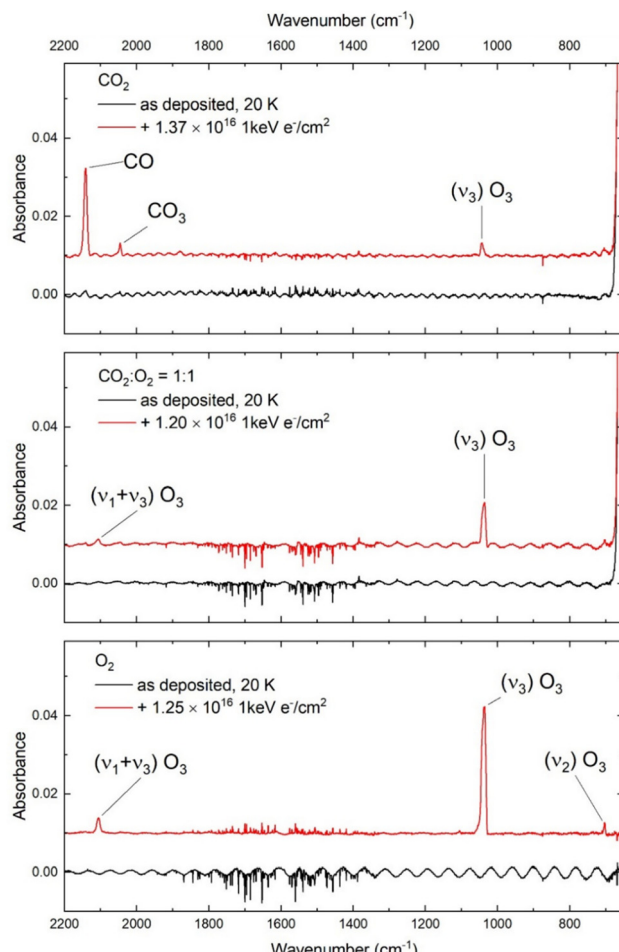


Fig. 2 Mid-infrared spectra of pristine and electron irradiated CO_2 , O_2 , and 1:1 mixed $\text{CO}_2:\text{O}_2$ astrophysical ice analogues. Products of radiation chemistry are indicated. Spectra are vertically offset for clarity. Oscillations in the baseline of the spectra are the result of interference effects, although these are not anticipated to influence our analyses.

insight into its formation. This absorption band is actually a composite structure of three features: the main absorption band due to monomeric O_3 centred at 1038 cm^{-1} is sandwiched between two satellite peaks at around 1042 and 1032 cm^{-1} attributed to the ozone dimer $[\text{O}_3 \cdots \text{O}_3]$ and the ozone-oxygen $[\text{O}_3 \cdots \text{O}]$ complexes, respectively^{37,38} (Fig. 3). Previous studies have suggested that the positions and profiles of the mid-infrared absorption bands of those species produced *via* the irradiation of mixed molecular ices may depend upon the initial stoichiometric composition of the ice,^{43–45} and our results suggest that this is also true with regards to the appearance of the asymmetric stretching mode (ν_3) of O_3 produced from electron irradiated $\text{CO}_2:\text{O}_2$ ices.

Examination of our post-irradiative mid-infrared spectra revealed that the three $\text{CO}_2:\text{O}_2$ mixed ices which were richest in O_2 (*i.e.*, the 0:1, 1:50, and 1:6 mixtures) resulted in a O_3 asymmetric stretching (ν_3) band which could be deconvoluted into three Gaussian sub-structures, indicating the presence of monomeric O_3 and of the $[\text{O}_3 \cdots \text{O}_3]$ and $[\text{O}_3 \cdots \text{O}]$ complexes (Fig. 4 and 5). All irradiated ices with a lower O_2 content (or,

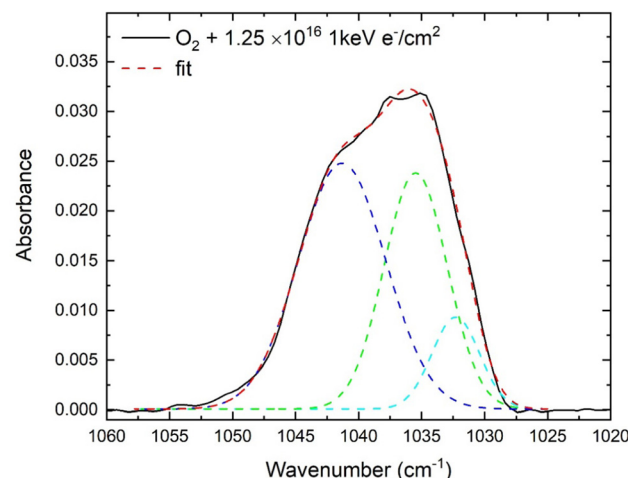


Fig. 3 Deconvolution of the O_3 asymmetric stretching (ν_3) mode as observed in an electron irradiated pure O_2 ice into its constituent Gaussian sub-structures. Similar deconvolutions were performed for all other analysed ices.

conversely, a higher CO_2 content) exhibited O_3 asymmetric stretching (ν_3) bands composed of only two Gaussian sub-structures, with that attributable to the $[\text{O}_3 \cdots \text{O}]$ complex being absent in the spectra of these ices. This is in line with the results of previous studies, which have reported the presence of the $[\text{O}_3 \cdots \text{O}]$ complex in an electron irradiated pure O_2 ice⁸ but not in an electron irradiated pure CO_2 ice.²¹

These observations may be directly related to the molecular environment in each irradiated ice, as free oxygen atoms are far more likely to be in the vicinity of (and thus, be able to complex with) a O_3 molecule in an irradiated O_2 ice than in an irradiated CO_2 ice. This is due to two reasons: firstly, the yield of free supra-thermal oxygen atoms from a dissociated O_2 molecule is

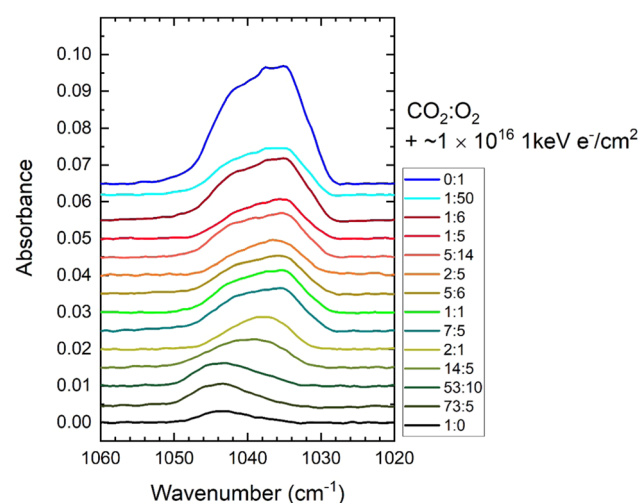


Fig. 4 Variation in the shape of the O_3 asymmetric stretching (ν_3) mode as observed in 1 keV electron irradiated ($1.3 \times 10^{16} \text{ e}^- \text{ cm}^{-2}$) $\text{CO}_2:\text{O}_2$ mixed ices of different stoichiometric compositions. Note that the scale on the y-axis is set to the 1:0 mixed ice, and that all other spectra are vertically offset for clarity.

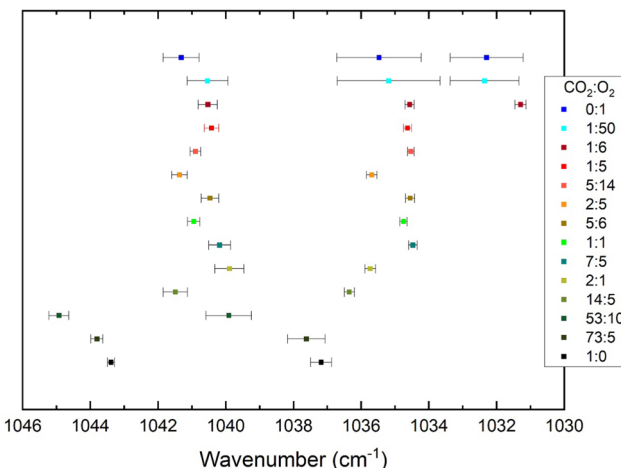


Fig. 5 Plot of the peak positions of the Gaussian sub-components of the O_3 asymmetric stretching (ν_3) mode in 1 keV electron irradiated $CO_2:O_2$ ices of different stoichiometries. Note that a peak for the $[O_3 \cdots O]$ sub-component was only detected in the three ices with the highest O_2 content.

twice that from a dissociated CO_2 molecule leading to a greater abundance of such atoms in a O_2 ice. Secondly, the formation of O_3 via the electron irradiation of O_2 ice only suffers from one competing reaction (the reformation of O_2) compared to its formation via the electron irradiation of CO_2 ice, for which many other competing reaction pathways are available which reduce the general abundance of O_3 available for co-ordination or complexation.²¹

The positions of the peaks of these band sub-structures were noted to vary from ice to ice, however a pattern is apparent in the case of the monomeric O_3 and $[O_3 \cdots O_3]$ peak positions. In the irradiated pure O_2 ices, these peaks are respectively located at 1035.5 and 1041.3 cm^{-1} , as shown in Fig. 5. On increasing the CO_2 content of the ice, these peaks appear to undergo a red-shift to lower wavenumbers, reaching 1034.6 and 1040.5 cm^{-1} in the $1:6$ $CO_2:O_2$ mixed ice, although we note that this observation may be a consequence of the comparatively higher uncertainties in the peak positions of the two ices richest in O_2 (Fig. 5). Further increases in the CO_2 content up to a stoichiometric ratio of $CO_2:O_2 = 7:5$ do not result in any noticeable changes in the position of these peaks (except for a slight blue-shift of the monomeric O_3 peak position in the $2:5$ $CO_2:O_2$ ice).

On moving to the next $CO_2:O_2$ ice in the series (*i.e.*, the $2:1$ mixture), however, it is possible to note that although the peak of the Gaussian sub-structure for the $[O_3 \cdots O_3]$ complex does not shift, that for the monomeric O_3 sub-structure experiences a blue-shift back to 1035.7 cm^{-1} ; similar to the position of this peak in the irradiated pure O_2 ice. Increasing the CO_2 content of the ice even further results in a blue-shift in the position of both peaks, which are located at 1039.9 and 1044.9 cm^{-1} in the $53:10$ $CO_2:O_2$ ice mixture. Finally, further increasing the CO_2 content of the ice results in these peaks undergoing another red-shift, where they are located at 1037.2 and 1043.4 cm^{-1} in the irradiated pure CO_2 ice (Fig. 5).

We note that, taken as a whole, the peak position of the O_3 asymmetric stretching mode (ν_3) blue-shifts from lower to

higher wavenumbers on increasing the CO_2 content of the electron irradiated binary $CO_2:O_2$ ices, with the exception of the three ices which were richest in CO_2 (*i.e.*, the $53:10$, $73:5$, and the $1:0$ mixtures) for which a ‘change of direction’ in the band peak position shifting is observed (Fig. 4 and 5). It is difficult to provide an exact explanation for these trends, although we note that experimental parameters such as optical thickness and molecular environments have been suggested to influence the O_3 asymmetric stretching (ν_3) band peak position.

Lastly, we review the O_3 productivity of each of the irradiated ices considered in this study. It is evident from eqn (3)–(6) that the successful electron-induced dissociation of a O_2 molecule is more efficient at yielding O_3 than is the dissociation of a CO_2 molecule due to the greater number of reaction pathways available to an irradiated CO_2 ice. Indeed, this has been borne out by the results of this study, as the molecular column density of O_3 (measured from the peak area of its asymmetric stretching (ν_3) band and taking A_ν to be $1.4 \times 10^{-17}\text{ cm molecule}^{-1}$ ²¹) observed in the irradiated pure O_2 ice was consistently higher than that observed in the pure CO_2 ice throughout irradiation (Fig. 6). This trend was also observed in the electron irradiated mixed $CO_2:O_2$ ices.

To better quantify the yield of O_3 as a result of the 1 keV electron irradiation of the ices considered in this study, we have defined a percentage formation efficiency based on a series of mass balance calculations which take into account the formation of radiolytic product molecules. Considering first the pure O_2 ice: the dissociation of one O_2 molecule results in the production of two oxygen atoms which may yield two O_3 product molecules as a result of their addition to (or insertion into) two neighbouring O_2 molecules. As such, the consumption of three O_2 molecules should yield two O_3 molecules (eqn (7)). Using a similar logic, the electron-induced dissociation of five CO_2 molecules should yield four CO , one CO_3 , and one O_3 molecules (eqn (8)). In the case of the $CO_2:O_2$ mixed ices, both mass

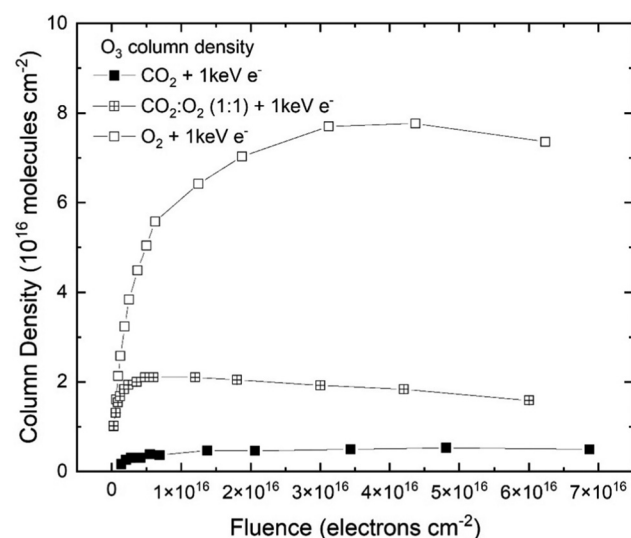
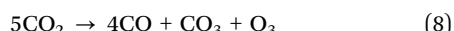


Fig. 6 Evolution of O_3 column density in electron irradiated pure O_2 , pure CO_2 , and $1:1$ mixed $CO_2:O_2$ ices plotted as a function of electron fluence.

balance equations are applicable and so eqn (7) and (8) may be added together.



The mass balance relations given in eqn (7) and (8), and that used for the mixed ices, are thus indicative of the O_3 formation pathways at their most efficient. Hence, by deriving O_3 as the subject of the formula in these equations and measuring the initial column densities of CO_2 and O_2 (in this particular case scaled to the maximum penetration depth of the incident electrons) before irradiation and the column densities of CO and CO_3 after a given fluence, the expected O_3 column density yield may be computed. By comparing this expected yield to the actual O_3 column density measured at that fluence, the percentage formation efficiency of the ice may be calculated fairly simply.

Fig. 7 depicts the O_3 formation efficiency of each ice considered in this study at a fluence of $10^{16} \text{ e}^- \text{ cm}^{-2}$. At this fluence, the column density of O_3 is approximately at its maximum in all but three ices: in the pure O_2 ice, the O_3 column density peaks at a later fluence (Fig. 6) while in the 2:1 and 2:5 mixed $\text{CO}_2:\text{O}_2$ ices, the peak O_3 column density occurs at a slightly earlier fluence. Nevertheless, the selected fluence arguably represents the best choice for our analysis of the O_3 production efficiency of each irradiated ice. As depicted by the hollow blue circles in Fig. 7, the pure O_2 ice was found to have

the highest O_3 formation efficiency at about 35%. This efficiency then progressively declines as the CO_2 content of the ice is raised, falling to about 15% when 25% of the ice is composed of CO_2 . Interestingly, further increases in the CO_2 content of the ice do not noticeably reduce the O_3 formation efficiency of the mixed ices as a result of their 1 keV electron irradiation until a CO_2 content of about 80% is reached, after which it declines steadily. The pure CO_2 ice has a O_3 formation efficiency of about 2%.

In order to ensure that the trend described above is robust and not dependent upon a particular selected definition of O_3 formation efficiency, we have re-analysed our data using a different definition for the latter; one based on the electron fluence yield of O_3 . As a reference, we have considered the case where one primary 1 keV electron dissociates one molecule in the target ice. We acknowledge that such a reference point is not representative of the actual physico-chemical mechanisms by which molecular dissociation in irradiated ices takes place which, as mentioned previously, is the result of the release of tens of thousands of low-energy ($< 20 \text{ eV}$) electrons.^{35,36,46} However, this reference point is convenient for assessing the O_3 formation efficiency of our irradiated ices as a function of primary electron fluence. Using this reference, a maximum of two O_3 molecules may be formed per incident electron during irradiation of the pure O_2 ice. Conversely, since three electron-induced molecular dissociations are required to generate the necessary number of free oxygen atoms to yield a single O_3 molecule during irradiation of a pure CO_2 ice, a maximum of one-third O_3 molecules per incident electron may be formed. The extension of this definition to the mixed ices is based on their stoichiometric composition.

Hence, using this definition, the reference column density of O_3 yielded as a result of electron irradiation is given as the mathematical product of the molecular formation rate per incident electron and the fluence at the maximum O_3 abundance in the ice. By comparing this reference column density with the column density of O_3 actually measured at this fluence, the percentage formation efficiency of each ice may be computed. As depicted by the black squares in Fig. 7, the O_3 formation efficiency trend across ice stoichiometric compositions calculated using the electron fluence yield definition is very similar to that calculated using the mass balance relations definition (depicted by blue hollow circles in Fig. 7). Indeed, most data point pairs are within about 10% of each other, thus indicating the robustness of this trend.

One noticeable discrepancy between the two trends is the O_3 formation efficiency of the electron irradiated pure O_2 ice, which is calculated to be about 35% when using the mass balance relations and about 90% when using the electron fluence yield definition. It should be noted, however, that the former percentage formation efficiency is very likely underestimated due to it having been calculated using molecular column densities measured when the O_3 abundance in the ice had not yet peaked (as explained previously), while the latter most likely indicates a possible upper bound efficiency.

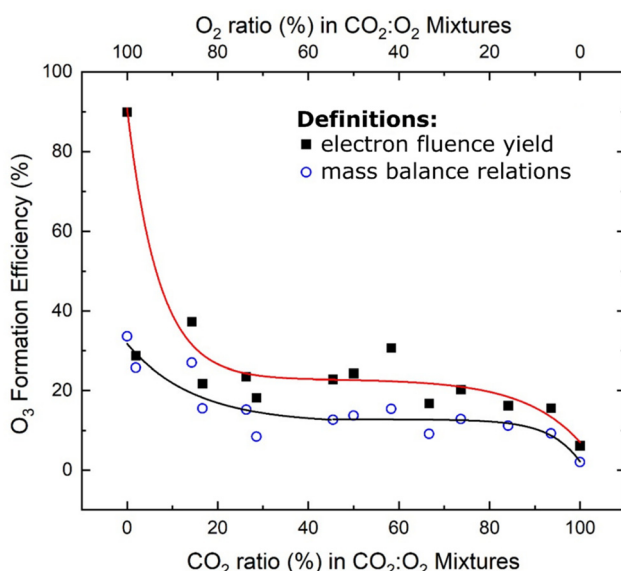


Fig. 7 Formation yield of O_3 (as a percentage) as a result of the 1 keV electron irradiation of the $\text{CO}_2:\text{O}_2$ ices considered in this study as calculated using the mass balance relations (hollow blue circles) and electron fluence yield (black squares) definitions. Error bars have been omitted, since the uncertainties are anticipated to be significantly lower than the systematic errors arising due to uncertainties associated with the band strength constant A_v used to calculate molecular column densities which, for mixed ices, could be as high as 50%. Each line represents the conjunction of two exponential fits joined at a percentage CO_2 content of 45%. Note that, in the case of the electron fluence yield definition, the fit does not include the 1:50 mixture.



4 Implications for Solar System chemistry

The work presented in this paper is directly applicable to the study of the chemistry of outer Solar System ices, particularly as it relates to the formation of O_3 . As has been previously noted, O_3 has been detected on a number of outer Solar System moons, including several of those of Jupiter and Saturn.^{2,3} We note that, on average, the surface temperatures of these moons are higher than the 20 K temperature at which irradiations were performed in this present study. However, temperature gradients across the lunar latitudes are well known, with polar regions being significantly colder than equatorial ones.⁴⁷ For example, temperatures as low as 23 K have been reported in the polar regions of Rhea during its long winter.⁴⁸

Moreover, several bodies in the Solar System (both inner and outer) with low axial tilts are known to possess permanently shadowed crater regions towards higher latitudes. The temperatures within these regions are significantly lower than the average surface temperature of the planet or moon, and thus allow for the condensation and accumulation of several otherwise volatile molecular species. In the furthest reaches of the Solar System, average surface temperatures are lower still, with volatile molecules such as N_2 or CH_4 being known to exist as solid ices on the surfaces of Pluto, Charon, and Triton.^{49,50} Thus, although our selected irradiation temperature of 20 K is representative of the lowest temperatures in the Solar System, it is still applicable to a wide variety of surface environments and the possible chemistry leading to O_3 formation occurring there.

The irradiation conditions presented in this study are also suitable for studying such chemistry, since the 1 keV electron irradiations described simulate the processing that such ices undergo as a result of their interaction with the solar wind or giant planetary magnetospheric plasmas. Indeed, the physico-chemical effects of magnetospheric ion and electron irradiation on the surfaces of the Jovian and Saturnian satellites have been well documented in the literature, and are thought to give rise to the formation of several new and potentially prebiotic molecules.^{22,51,52} As such, our experimental conditions allow us to interpret our results in terms of potential magnetospheric plasma-driven O_3 synthesis occurring on the surfaces of several of the moons of Jupiter, Saturn, and Uranus.

4.1 The icy moons of Jupiter

Of the four major (Galilean) moons of Jupiter, the presence of O_3 has only been confirmed on Ganymede,² where the highest molecular abundance is located on the moon's trailing side consistent with observations of icy O_2 and with the preferential irradiation by magnetospheric charged particles.^{53,54} As such, it is expected that the bulk of the O_3 present on Ganymede is sourced from the irradiation of the surface O_2 ices.[†] However, CO_2 has also been detected at the surface,⁵⁵ and so it is possible

[†] It should be noted that, unlike the other Galilean satellites, Ganymede possesses its own magnetosphere, and so the flux of incoming charged particles is expected to be significantly attenuated in equatorial regions. Nevertheless, radiation chemistry is still expected to play a key role in the chemical alteration of the lunar surface in these regions.

that O_3 could also be sourced *via* the irradiation of this molecule,²¹ although the results of this study combined with the relative distributions of O_2 and CO_2 at the surface of Ganymede suggest that this contribution is likely to be a minor one.

No O_3 has yet been detected on Europa or Callisto, despite the known presence of O_2 on both of these moons.⁵⁶ The results of this study (as well as those of previous works) demonstrate that the formation of O_3 from irradiated O_2 ices is rather efficient, and so the non-detection of O_3 on these icy moons is somewhat surprising. Loeffler and Hudson⁴ have suggested that this lack of O_3 may be due to its consumption during the oxidation of other molecular species, such as SO_2 . Similar arguments have been suggested to explain the non-detection of O_3 in cometary and interstellar ices. Forthcoming interplanetary missions to the Jovian moon system, such as the ESA *Jupiter Icy Moons Explorer* and NASA *Europa Clipper* missions^{26,27} may detect O_3 in observed surface patches of isolated O_2 or CO_2 exposed to incident magnetospheric plasma, and our spectroscopic results may therefore prove useful in confirming its presence there.

4.2 The icy moons of Saturn and Uranus

All the major moons of Saturn (with the notable exceptions of Titan and Iapetus) are characterised by surfaces dominated by H_2O ices. The detections of O_3 on the surfaces of Rhea and Dione³ therefore provide a challenge, as laboratory studies have thus far been largely unsuccessful in documenting any appreciable yield of O_3 as a result of the irradiation of H_2O ices, mainly due to the known catalytic role of OH radicals in the destruction of O_3 .⁵⁷ However, CO_2 is known to be present on the surfaces of both of these moons,^{58,59} and so its irradiation is a more likely source for the observed O_3 . This radiation chemistry, driven by the interaction of the lunar surfaces with the Saturnian magnetosphere, is also thought to sustain a tenuous exosphere composed of CO_2 and O_2 on Rhea.²⁵ Our irradiations of CO_2 -rich ices in this present study therefore provide a good analogue of the surface processes occurring on Rhea and Dione.

The synthesis of O_3 from electron irradiated CO_2 -rich CO_2 : O_2 ice mixtures as demonstrated in this study is also applicable to several of the major satellites of Uranus. The surfaces of these moons are composed of a mixture of H_2O ice and dark, carbon-rich refractory material.⁶⁰ Laboratory experiments have already demonstrated that the irradiation of such materials gives rise to the formation of CO and CO_2 molecules.^{61,62} Indeed, CO_2 ice has been firmly detected at the surfaces of Umbriel and Ariel, and tentatively detected at the surfaces of Titania and Oberon.^{63–65} CO_2 ices there may also be intermixed with smaller quantities of non-native O_2 ice sourced from the charged particle and ultraviolet photon irradiation of the surface.⁶⁶ As such, our experimental results suggest that there should be some O_3 formed at the surfaces of these moons as a result of their interaction with the Uranian magnetosphere.

4.3 Ozone on the moon

Generally speaking, the surface of the Earth's moon is depleted in volatiles.⁶⁷ Nevertheless, ices are known to exist there



especially within the permanently shadowed regions at the lunar poles. Data collected by the Chandra Altitudinal Composition Explorer (CHACE) instrument on the ISRO *Moon Impact Probe* has shown that oxygen-rich species are prevalent in the lunar exosphere,⁶⁸ while data from the NASA *Lunar Crater Observation and Sensing Satellite* (LCROSS) has revealed that the same is true for the surface ices.⁶⁹ The presence of such species in a radiation environment mediated by the solar wind means that the presence of O₃ is also likely (as demonstrated by this and previous studies), although this has yet to be confirmed.⁷⁰ As such, our experiments are also representative of possible O₃ formation processes in these permanently shadowed regions at the lunar poles.

5 Conclusions

In this study, the 1 keV electron irradiation of a series of stoichiometrically distinct CO₂:O₂ astrophysical ice analogues, including the two pure end-members and 12 binary mixtures, has been studied in detail. Such irradiations are representative of the radiation chemistry occurring in various icy outer Solar System environments. We have been able to successfully quantify the O₃ productivity of these ice mixtures as a result of their irradiation, and have determined that the formation efficiency of this species decreases upon the introduction of CO₂ to a pure O₂ ice. Once the CO₂ content of the ice reaches 25%, further additions of CO₂ do not noticeably decrease the O₃ formation efficiency until a CO₂ content of about 70–80% is reached, after which this efficiency declines further.

Using mid-infrared spectroscopy, we have also been able to perform a characterisation of the O₃ asymmetric stretching mode (ν_3) in each of the electron irradiated ices. In the three ices richest in O₂, this absorption mode may be deconvoluted into three Gaussian sub-structures, indicating the presence of monomeric O₃, as well as the [O₃···O₃] and [O₃···O] complexes. In ices containing a higher CO₂ content, no spectroscopic evidence for the latter complex was observed. Such results may prove useful in the interpretation of data collected by forthcoming interplanetary missions, and may provide an insight into the formation mechanism of the O₃ already observed on several outer Solar System bodies.

Author contributions

The experiment was designed by Sergio Ioppolo, Zuzana Kaňuchová, and Alejandra Traspas Muiña and was carried out by Duncan V. Mifsud, Péter Herczku, Béla Sulik, Sándor T. S. Kovács, and Zoltán Juhász. Data analysis was performed by Zuzana Kaňuchová, Duncan V. Mifsud, and Sergio Ioppolo. Duncan V. Mifsud and Zuzana Kaňuchová prepared the manuscript. All authors took part in discussions relating to the interpretation of the results and the improvement of the manuscript.

Conflicts of interest

The authors declare that they have no known competing financial interests or personal relationships that could have appeared to influence the work reported in this paper.

Acknowledgements

The authors all gratefully acknowledge funding from the Europlanet 2024 RI which has received funding from the European Union Horizon 2020 Research Innovation Programme under grant agreement No. 871149. The main components of the ICA set-up were purchased with funding from the Royal Society through grants UF130409, RGF/EA/180306, and URF/R/191018. Recent developments of the installation were also supported in part by the Eötvös Loránd Research network *via* grants ELKH IF-2/2019 and ELKH IF-5/2020. Support has also been received from the National Research, Development, and Innovation Fund of Hungary through grant No. K128621. Duncan V. Mifsud is the grateful recipient of a University of Kent Vice-Chancellor's Research Scholarship. The research of Zuzana Kaňuchová is supported by VEGA – the Slovak Grant Agency for Science (grant No. 2/0059/22) and the Slovak Research and Development Agency (contract No. APVV-19-0072). Sergio Ioppolo acknowledges the Royal Society for financial support. Alejandra Traspas Muiña thanks Queen Mary University of London for doctoral funding.

References

- 1 J. Staehelin, N. R. P. Harris, C. Appenzeller and J. Eberhard, *Rev. Geophys.*, 2001, **39**, 231, DOI: [10.1029/1999RG000059](https://doi.org/10.1029/1999RG000059).
- 2 K. S. Noll, R. E. Johnson, A. L. Lane, D. L. Domingue and H. A. Weaver, *Science*, 1996, **273**, 341, DOI: [10.1126/science.273.5273.341](https://doi.org/10.1126/science.273.5273.341).
- 3 K. S. Noll, T. L. Roush, D. P. Cruikshank, R. E. Johnson and Y. J. Pendleton, *Nature*, 1997, **388**, 45, DOI: [10.1038/40348](https://doi.org/10.1038/40348).
- 4 M. J. Loeffler and R. L. Hudson, *Astrophys. J., Lett.*, 2016, **833**, L9, DOI: [10.3847/2041-8213/833/1/L9](https://doi.org/10.3847/2041-8213/833/1/L9).
- 5 A. Bieler, K. Altweig, H. Balsiger, A. Bar-Nun, J.-J. Berthelier, P. Bochsler, C. Briois, U. Calmonte, M. Combi, J. De Keyser, E. F. van Dishoeck, B. Fiethe, S. A. Fuselier, S. Gasc, T. I. Gombosi, K. C. Hansen, M. Hässig, A. Jäckel, E. Kopp, A. Korth, L. Le Roy, U. Mall, R. Maggiolo, B. Marty, O. Mousis, T. Owen, H. Rème, M. Rubin, T. Sémon, C.-Y. Tzou, J. H. Waite, C. Walsh and P. Wurz, *Nature*, 2015, **526**, 678, DOI: [10.1038/nature15707](https://doi.org/10.1038/nature15707).
- 6 M. Rubin, K. Altweig, E. F. van Dishoeck and G. Schewe, *Astrophys. J., Lett.*, 2015, **815**, L11, DOI: [10.1088/2041-8205/815/1/L11](https://doi.org/10.1088/2041-8205/815/1/L11).
- 7 C. J. Bennett and R. I. Kaiser, *Astrophys. J.*, 2005, **635**, 1362, DOI: [10.1086/497618](https://doi.org/10.1086/497618).
- 8 B. Sivaraman, C. S. Jamieson, N. J. Mason and R. I. Kaiser, *Astrophys. J.*, 2007, **669**, 1414, DOI: [10.1086/521216](https://doi.org/10.1086/521216).
- 9 C. P. Ennis, C. J. Bennett and R. I. Kaiser, *Phys. Chem. Chem. Phys.*, 2011, **13**, 9469, DOI: [10.1039/C1CP20434C](https://doi.org/10.1039/C1CP20434C).

10 U. Raut, M. J. Loeffler, M. Famá and R. A. Baragiola, *J. Chem. Phys.*, 2011, **134**, 194501, DOI: [10.1063/1.3589201](https://doi.org/10.1063/1.3589201).

11 C. P. Ennis and R. I. Kaiser, *Astrophys. J.*, 2012, **745**, 103, DOI: [10.1088/0004-637X/745/2/103](https://doi.org/10.1088/0004-637X/745/2/103).

12 C. J. Bennett, C. P. Ennis and R. I. Kaiser, *Astrophys. J.*, 2014, **782**, 63, DOI: [10.1088/0004-637X/782/2/63](https://doi.org/10.1088/0004-637X/782/2/63).

13 J. Zhen and H. Linnartz, *Mon. Not. R. Astron. Soc.*, 2014, **437**, 3190, DOI: [10.1093/mnras/stt2106](https://doi.org/10.1093/mnras/stt2106).

14 P. Boduch, R. Brunetto, J. J. Ding, A. Domaracka, Z. Kaňuchová, M. E. Palumbo, H. Rothard and G. Strazzulla, *Icarus*, 2016, **277**, 424, DOI: [10.1016/j.icarus.2016.05.026](https://doi.org/10.1016/j.icarus.2016.05.026).

15 S. Ioppolo, Z. Kaňuchová, R. L. James, A. Dawes, N. C. Jones, S. V. Hoffmann, N. J. Mason and G. Strazzulla, *Astron. Astrophys.*, 2020, **641**, A154, DOI: [10.1051/0004-6361/201935477](https://doi.org/10.1051/0004-6361/201935477).

16 B. Sivaraman, B. N. Rajasekhar, D. Fulvio, A. Hunniford, R. W. McCullough, M. E. Palumbo and N. J. Mason, *J. Chem. Phys.*, 2013, **139**, 074706, DOI: [10.1063/1.4818166](https://doi.org/10.1063/1.4818166).

17 C. J. Bennett, C. P. Ennis and R. I. Kaiser, *Astrophys. J.*, 2014, **794**, 57, DOI: [10.1088/0004-637X/794/1/57](https://doi.org/10.1088/0004-637X/794/1/57).

18 X. Y. Lv, P. Boduch, J. J. Ding, A. Domaracka, T. Langlinay, M. E. Palumbo, H. Rothard and G. Strazzulla, *Mon. Not. R. Astron. Soc.*, 2014, **438**, 922, DOI: [10.1093/mnras/stt2004](https://doi.org/10.1093/mnras/stt2004).

19 C. Mejía, M. Bender, D. Severin, C. Trautmann, P. Boduch, V. Bordalo, A. Domaracka, X. Y. Lv, R. Martinez and H. Rothard, *Nucl. Instrum. Meth. Phys. Res. B*, 2015, **365**, 477, DOI: [10.1016/j.nimb.2015.09.039](https://doi.org/10.1016/j.nimb.2015.09.039).

20 R. Martín-Doménech, J. Manzano-Santamaría, G. M. Muñoz-Caro, G. A. Cruz-Díaz, Y.-J. Chen, V. J. Herrero and I. Tanarro, *Astron. Astrophys.*, 2015, **584**, 14, DOI: [10.1051/0004-6361/201526003](https://doi.org/10.1051/0004-6361/201526003).

21 D. V. Mifsud, Z. Kaňuchová, S. Ioppolo, P. Herczku, A. Traspas Muiña, T. A. Field, P. A. Hailey, Z. Juhász, S. T. S. Kovács, N. J. Mason, R. W. McCullough, S. Pavithraa, K. K. Rahul, B. Paripás, B. Sulik, S.-L. Chou, J.-I. Lo, A. Das, B.-M. Cheng, B. N. Rajasekhar, A. Bhardwaj and B. Sivaraman, *J. Mol. Spectrosc.*, 2022, **385**, 111599, DOI: [10.1016/j.jms.2022.111599](https://doi.org/10.1016/j.jms.2022.111599).

22 T. Cassidy, P. Coll, F. Raulin, R. W. Carlson, R. E. Johnson, M. J. Loeffler, K. P. Hand and R. A. Baragiola, *Space Sci. Rev.*, 2010, **153**, 299, DOI: [10.1007/s11214-009-9625-3](https://doi.org/10.1007/s11214-009-9625-3).

23 M. Läuter, T. Kramer, M. Rubin and K. Altwegg, *Mon. Not. R. Astron. Soc.*, 2019, **483**, 852, DOI: [10.1093/mnras/sty3103](https://doi.org/10.1093/mnras/sty3103).

24 M. Combi, Y. Shou, N. Fougere, V. Tenishev, K. Altwegg, M. Rubin, D. Bockelée-Morvan, F. Capaccioni, Y.-C. Cheng, U. Fink, T. Gombosi, K. C. Hansen, Z. Huang, D. Marshall and G. Toth, *Icarus*, 2020, **335**, 113421, DOI: [10.1016/j.icarus.2019.113421](https://doi.org/10.1016/j.icarus.2019.113421).

25 B. D. Teolis, G. H. Jones, P. F. Miles, R. L. Tokar, B. A. Magee, J. H. Waite, E. Roussos, D. T. Young, F. J. Crary, A. J. Coates, R. E. Johnson, W.-L. Tseng and R. A. Baragiola, *Science*, 2010, **330**, 1813, DOI: [10.1126/science.1198366](https://doi.org/10.1126/science.1198366).

26 O. Grasset, M. K. Dougherty, A. Coustenis, E. J. Bunce, C. Erd, D. Titov, M. Blanc, A. Coates, P. Drossart, L. N. Fletcher, H. Hussmann, R. Jaumann, N. Krupp, J.-P. Lebreton, O. Prieto-Ballesteros, P. Tortora, F. Tosi and T. van Hoolst, *Planet. Space Sci.*, 2013, **78**, 1, DOI: [10.1016/j.pss.2012.12.002](https://doi.org/10.1016/j.pss.2012.12.002).

27 C. B. Phillips and R. T. Pappalardo, *Eos Trans. Am. Geophys. Union*, 2014, **95**, 165, DOI: [10.1002/2014EO200002](https://doi.org/10.1002/2014EO200002).

28 J. P. Gardner, J. C. Mather, M. Clampin, R. Doyon, M. A. Greenhouse, H. B. Hammel, J. B. Hutchings, P. Jakobsen, S. J. Lilly, K. S. Long, J. I. Lunine, M. J. McCaughrean, M. Mountain, J. Nella, G. H. Rieke, M. J. Rieke, H.-W. Rix, E. P. Smith, G. Sonneborn, M. Stiavelli, H. S. Stockman, R. A. Windhorst and G. S. Wright, *Space Sci. Rev.*, 2006, **123**, 485, DOI: [10.1007/s11214-006-8315-7](https://doi.org/10.1007/s11214-006-8315-7).

29 P. Herczku, D. V. Mifsud, S. Ioppolo, Z. Juhász, Z. Kaňuchová, S. T. S. Kovács, A. Traspas Muiña, P. A. Hailey, I. Rajta, I. Vajda, N. J. Mason, R. W. McCullough, B. Paripás and B. Sulik, *Rev. Sci. Instrum.*, 2021, **92**, 084501, DOI: [10.1063/5.0050930](https://doi.org/10.1063/5.0050930).

30 D. V. Mifsud, Z. Juhász, P. Herczku, S. T. S. Kovács, S. Ioppolo, Z. Kaňuchová, M. Czentye, P. A. Hailey, A. Traspas Muiña, N. J. Mason, R. W. McCullough, B. Paripás and B. Sulik, *Eur. Phys. J. D*, 2021, **75**, 182, DOI: [10.1140/epjd/s10053-021-00192-7](https://doi.org/10.1140/epjd/s10053-021-00192-7).

31 P. A. Gerakines, W. A. Schutte, J. M. Greenberg and E. F. van Dishoeck, *Astron. Astrophys.*, 1995, **296**, 810.

32 R. Luna, M. Á. Satorre, M. Domingo, C. Millán and C. Santonja, *Icarus*, 2012, **221**, 186, DOI: [10.1016/j.icarus.2012.07.016](https://doi.org/10.1016/j.icarus.2012.07.016).

33 D. Fulvio, B. Sivaraman, G. A. Baratta, M. E. Palumbo and N. J. Mason, *Spectrochim. Acta, Part A*, 2009, **72**, 1007, DOI: [10.1016/j.saa.2008.12.030](https://doi.org/10.1016/j.saa.2008.12.030).

34 D. Drouin, A. R. Couture, D. Joly, X. Tastet, V. Aimez and R. Gauvin, *Scanning*, 2007, **29**, 92, DOI: [10.1002/sca.20000](https://doi.org/10.1002/sca.20000).

35 N. J. Mason, B. Nair, S. Jheeta and E. Szymańska, *Faraday Discuss.*, 2014, **168**, 235, DOI: [10.1039/C4FD00004H](https://doi.org/10.1039/C4FD00004H).

36 M. C. Boyer, N. Rivas, A. A. Tran, C. A. Verish and C. R. Arumainayagam, *Surf. Sci.*, 2016, **652**, 26, DOI: [10.1016/j.susc.2016.03.012](https://doi.org/10.1016/j.susc.2016.03.012).

37 M. Bahou, L. Schriver-Mazzuoli and A. Schriver, *J. Chem. Phys.*, 2001, **114**, 4045, DOI: [10.1063/1.1342223](https://doi.org/10.1063/1.1342223).

38 H. Chaabouni, L. Schriver-Mazzuoli and A. Schriver, *J. Phys. Chem. A*, 2000, **104**, 6962, DOI: [10.1021/jp0008290](https://doi.org/10.1021/jp0008290).

39 H. Chaabouni, L. Schriver-Mazzuoli and A. Schriver, *Low Temp. Phys.*, 2000, **26**, 712, DOI: [10.1063/1.1312398](https://doi.org/10.1063/1.1312398).

40 P. C. Cosby, *J. Chem. Phys.*, 1993, **98**, 9560, DOI: [10.1063/1.464387](https://doi.org/10.1063/1.464387).

41 A. S. Morillo-Candas, T. Silva, B. L. M. Klarenaar, M. Grofulović, V. Guerra and O. Guaitella, *Plasma Sources Sci. Technol.*, 2020, **29**, 01LT01, DOI: [10.1088/1361-6595/ab6075](https://doi.org/10.1088/1361-6595/ab6075).

42 S. Ioppolo, H. M. Cuppen, C. Romanzin, E. F. van Dishoeck and H. Linnartz, *Astrophys. J.*, 2008, **686**, 1474, DOI: [10.1086/591506](https://doi.org/10.1086/591506).

43 M. H. Moore, R. L. Hudson and R. W. Carlson, *Icarus*, 2007, **189**, 409, DOI: [10.1016/j.icarus.2007.01.018](https://doi.org/10.1016/j.icarus.2007.01.018).

44 Z. Kaňuchová, P. Boduch, A. Domaracka, M. E. Palumbo, H. Rothard and G. Strazzulla, *Astron. Astrophys.*, 2017, **604**, A68, DOI: [10.1051/0004-6361/201730711](https://doi.org/10.1051/0004-6361/201730711).

45 C. Mejía, A. L. F. de Barros, H. Rothard, P. Boduch and E. F. da Silveira, *Astrophys. J.*, 2020, **894**, 132, DOI: [10.3847/1538-4357/ab8935](https://doi.org/10.3847/1538-4357/ab8935).



46 S. M. Pimblott and J. A. LaVerne, *Radiat. Phys. Chem.*, 2007, **76**, 1244, DOI: [10.1016/j.radphyschem.2007.02.012](https://doi.org/10.1016/j.radphyschem.2007.02.012).

47 Y. Ashkenazy, *Heliyon*, 2019, **5**, e01908, DOI: [10.1016/j.heliyon.2019.e01908](https://doi.org/10.1016/j.heliyon.2019.e01908).

48 C. J. A. Howett, J. R. Spencer, T. Hurford, A. Verbiscer and M. Segura, *Icarus*, 2016, **272**, 140, DOI: [10.1016/j.icarus.2016.02.033](https://doi.org/10.1016/j.icarus.2016.02.033).

49 D. P. Cruikshank, T. L. Roush, T. C. Owen, T. R. Geballe, C. De Bergh, B. Schmitt, R. H. Brown and M. J. Bartholomew, *Science*, 1993, **261**, 742, DOI: [10.1126/science.261.5122.742](https://doi.org/10.1126/science.261.5122.742).

50 W. M. Grundy, R. P. Binzel, B. J. Buratti, J. C. Cook, D. P. Cruikshank, C. M. Dalle Ore, A. M. Earle, K. Ennico, C. J. A. Howett, A. W. Lunsford, C. B. Olkin, A. H. Parker, S. Philippe, S. Protopapa, E. Quirico, D. C. Reuter, B. Schmitt, K. N. Singer, A. J. Verbiscer, R. A. Beyer, M. W. Buie, A. F. Cheng, D. E. Jennings, I. R. Linscott, J. W. M. Parker, P. M. Schenk, J. R. Spencer, J. A. Stansberry, S. A. Stern, H. B. Throop, C. C. C. Tsang, H. A. Weaver, G. E. Weigle II, L. A. Young and the New Horizons Science Team, *Science*, 2016, **351**, aad9189, DOI: [10.1126/science.aad9189](https://doi.org/10.1126/science.aad9189).

51 G. Strazzulla and M. E. Palumbo, *Planet. Space Sci.*, 1998, **46**, 1339, DOI: [10.1016/S0032-0633\(97\)00210-9](https://doi.org/10.1016/S0032-0633(97)00210-9).

52 L. R. Dartnell, *Astrobiology*, 2011, **11**, 551, DOI: [10.1089/ast.2010.0528](https://doi.org/10.1089/ast.2010.0528).

53 J. R. Spencer, W. M. Calvin and M. J. Person, *J. Geophys. Res.: Planets*, 1995, **100**, 19049, DOI: [10.1029/95JE01503](https://doi.org/10.1029/95JE01503).

54 W. M. Calvin, R. E. Johnson and J. R. Spencer, *Geophys. Res. Lett.*, 1996, **23**, 673, DOI: [10.1029/96GL00450](https://doi.org/10.1029/96GL00450).

55 C. A. Hibbitts, R. T. Pappalardo, G. B. Hansen and T. B. McCord, *J. Geophys. Res.: Planets*, 2003, **108**, 5036, DOI: [10.1029/2002JE001956](https://doi.org/10.1029/2002JE001956).

56 J. R. Spencer and W. M. Calvin, *Astron. J.*, 2002, **124**, 3400, DOI: [10.1086/344307](https://doi.org/10.1086/344307).

57 P. Boduch, E. F. da Silveira, A. Domaracka, O. Gomis, X. Y. Lv, M. E. Palumbo, S. Pilling, H. Rothard, E. Seperuelo Duarte and G. Strazzulla, *Adv. Astron.*, 2011, **2011**, 327641, DOI: [10.1155/2011/327641](https://doi.org/10.1155/2011/327641).

58 F. Scipioni, F. Tosi, K. Stephan, G. Filacchione, M. Ciarniello, F. Capaccioni, P. Cerroni and the VIMS Team, *Icarus*, 2013, **226**, 1331, DOI: [10.1016/j.icarus.2013.08.008](https://doi.org/10.1016/j.icarus.2013.08.008).

59 F. Scipioni, F. Tosi, K. Stephan, G. Filacchione, M. Ciarniello, F. Capaccioni, P. Cerroni and the VIMS Team, *Icarus*, 2014, **234**, 1, DOI: [10.1016/j.icarus.2014.02.010](https://doi.org/10.1016/j.icarus.2014.02.010).

60 R. J. Cartwright, J. P. Emery, A. S. Rivkin, D. E. Trilling and N. Pinilla-Alonso, *Icarus*, 2015, **257**, 428, DOI: [10.1016/j.icarus.2015.05.020](https://doi.org/10.1016/j.icarus.2015.05.020).

61 V. Mennella, M. E. Palumbo and G. A. Baratta, *Astrophys. J.*, 2004, **615**, 1073, DOI: [10.1086/424685](https://doi.org/10.1086/424685).

62 V. Mennella, G. A. Baratta, M. E. Palumbo and E. A. Bergin, *Astrophys. J.*, 2006, **643**, 923, DOI: [10.1086/502965](https://doi.org/10.1086/502965).

63 W. M. Grundy, L. A. Young, J. R. Spencer, R. E. Johnson, E. F. Young and M. W. Buie, *Icarus*, 2006, **184**, 543, DOI: [10.1016/j.icarus.2006.04.016](https://doi.org/10.1016/j.icarus.2006.04.016).

64 W. M. Grundy, L. A. Young and E. F. Young, *Icarus*, 2003, **162**, 222, DOI: [10.1016/S0019-1035\(02\)00075-1](https://doi.org/10.1016/S0019-1035(02)00075-1).

65 M. M. Sori, J. Bapst, A. M. Bramson, S. Byrne and M. E. Landis, *Icarus*, 2017, **290**, 1, DOI: [10.1016/j.icarus.2017.02.029](https://doi.org/10.1016/j.icarus.2017.02.029).

66 C. Ahrens, H. Meraviglia and C. Bennett, *Geosci.*, 2022, **12**, 51, DOI: [10.3390/geosciences12020051](https://doi.org/10.3390/geosciences12020051).

67 P. G. Lucey, N. Petro, D. M. Hurley, W. M. Farrell, P. Prem, E. S. Costello, M. L. Cable, M. K. Barker, M. Benna, M. D. Dyar, E. A. Fisher, R. O. Green, P. O. Hayne, K. Hibbitts, C. Honniball, S. Li, E. Malaret, K. Mandt, E. Mazarico, M. McCanta, C. Pieters, X. Sun, D. Thompson and T. Orlando, *Geochem.*, 2021, 125858, DOI: [10.1016/j.chemer.2021.125858](https://doi.org/10.1016/j.chemer.2021.125858).

68 R. Sridharan, S. M. Ahmed, T. P. Das, P. Sreelatha, P. Pradeepkumar, N. Naik and G. Supriya, *Planet. Space Sci.*, 2010, **58**, 947, DOI: [10.1016/j.pss.2010.02.013](https://doi.org/10.1016/j.pss.2010.02.013).

69 A. Colaprete, P. Schultz, J. Heldmann, D. Wooden, M. Shirley, K. Ennico, B. Hermalyn, W. Marshall, A. Ricco, R. C. Elphic, D. Goldstein, D. Summy, G. D. Bart, E. Asphaug, D. Korycansky, D. Landis and L. Sollitt, *Science*, 2010, **330**, 463, DOI: [10.1126/science.1186986](https://doi.org/10.1126/science.1186986).

70 B. Sivaraman, B. G. Nair, B. N. Rajasekhar, J.-I. Lo, R. Sridharan, B.-M. Cheng and N. J. Mason, *Chem. Phys. Lett.*, 2014, **603**, 33, DOI: [10.1016/j.cplett.2014.04.021](https://doi.org/10.1016/j.cplett.2014.04.021).

